Advanced Composite Materials
Publication details, including instructions for authors and subscription information:
http://www.tandfonline.com/loi/tacm20

Vibration control of a smart structure embedded with metal-core piezoelectric fibers

Kiyoshi Takagi , Hiroshi Sato & Muneharu Saigo
Version of record first published: 02 Apr 2012.

To cite this article: Kiyoshi Takagi , Hiroshi Sato & Muneharu Saigo (2006): Vibration control of a smart structure embedded with metal-core piezoelectric fibers, Advanced Composite Materials, 15:4, 403-417

To link to this article: http://dx.doi.org/10.1163/156855106778835195

Adv. Composite Mater., Vol. 15, No. 4, pp. 403–417 (2006)

Also available online - www.brill.nl/acm

Vibration control of a smart structure embedded with metal-core piezoelectric fibers

KIYOSHI TAKAGI *, HIROSHI SATO and MUNEHARU SAIGO

Advanced Manufacturing Research Institute, National Institute of Advanced Industrial Science and Technology (AIST), 1-2-1 Namiki Tsukuba, Ibaraki, Japan

Received 1 November 2005; accepted 30 November 2005

Abstract—This paper addresses the active vibration control of a new smart board designed by mounting piezoelectric fibers with a metal core on the surface of the CFRP composite. These complex fibers function as sensors and actuators in the CFRP board. A finite-element model of a cantilever and a reduced order model for controller design were established. The piezoelectric fibers are uneven in the actuator outputs. Therefore, a linear fractional transformation (LFT) is formulated considering the unevenness of the actuator outputs as the perturbation. Next, the controller is designed by using μ synthesis, considering the perturbation and robust stability. The control performance of the proposed method is verified by experiment and demonstrates that piezoelectric fibers can be effectively used in vibration control.

Keywords: Vibration control; smart structure; metal core piezoelectric fiber; μ synthesis.

NOMENCLATURE

l	length of the beam [m]
E	modulus of elasticity of the beam [Pa]
t_b	thickness of the beam [m]
w_b	width of the beam [m]
m	line density of the beam [kg]
r	radius of the piezoelectric fiber [m]
r_c	radius of the metal core [m]
h	distance between neutral axis and center of piezoelectric fiber [m]

*To whom correspondence should be addressed. E-mail: takagi.k@aist.go.jp
Edited by the JSCM

E_a	modulus of elasticity of the piezoelectric fiber without core [Pa]
E_p	modulus of elasticity of metal core [Pa]
d_{31}	piezoelectric constant (strain/field) [m/V]
C_p	capacitance of the piezoelectric fiber [F]
z_f	distance between a point on the outer circumference of the piezoelectric fiber and the y-axis [m]
z_c	distance between a point on the outer circumference of the metal core and the y-axis [m]

1. INTRODUCTION

Research and application of smart structures where actuators and sensors are consistent with the main structures have been conducted for ten years. The smart structures are capable of damage detection and control to avoid a fatal collapse of the structure. The capability of smart structures to sense and control damage leads to a wide range of potential applications, including vibration suppression of aircraft structures, and shape control of large space trusses. Studies have been performed on the vibration control of smart beams consisting of a composite substrate and piezoelectric patches bonded to the substrate's surface [1]. Examples include vibration control using a self-sensing piezoelectric actuator [2, 3] and the placement optimization of multiple piezoelectric actuators [4].

In embedding piezoelectric materials in composite materials such as CFRP, the sensor and actuator shapes must be considered to minimize harmful influences on the mechanical performance of the composite material. As one solution, the Active Materials and Structures Laboratory at MIT proposed using piezoelectric material in fiber shape [5]. In their research, thin PZT fibers are transversely aligned in a polymer matrix, and the fiber laminates are put between interdigital electrodes (IDT) at right angles to gain a larger strain of d_{33} mode along the fiber axis. These fibers are strong and, conformable, and therefore can be used in commercial products such as ski boards and tennis rackets to suppress the vibration. However, these fibers have disadvantages, as IDT is necessary for their use as sensors and actuators and the fragility of ceramics is in question. Therefore, one of the authors has proposed a complex piezoelectric fiber consisting of fine metal wire coated with PZT ceramics (piezoelectric fiber with metal core) [7]. Piezoelectric fibers with metal cores have at least three advantages. (1) They do not required electrodes, since the metal core in the fiber is one electrode and the CFRP matrix can be used as a ground electrode. (2) They resist breakage, because the metal core overcomes the fragility. (3) They are highly resistant to external noise. Because our fiber is embedded in a CFRP composite with high electrical conductivity, the CFRP composite easily blocks external noise. Moreover, passive vibration control of a smart beam equipped

with these fibers can be achieved by using a shunted circuit. However, it is difficult to suppress vibrations effectively because of the low capacitance of the fibers [8].

This paper discusses the active vibration control of a smart beam having piezoelectric fibers with metal cores where they function as sensors and actuators in the CFRP composite. However, multiple piezoelectric fibers are embedded to gain more actuator power, creating unevenness in the actuator outputs. Unevenness of the actuator outputs degrades the control performance when all fibers are driven with a single piezo amplifier. Hence, we designed a controller using μ synthesis considering the actuator unevenness. First, we established a finite-element model of a cantilever beam embedded with the piezoelectric fiber and a reduced-order model for controller design. We next transformed the reduced-order model into a linear fractional transformation (LFT) representation considering the actuator unevenness as the perturbation. Next, using the controller designed by using μ synthesis, control experiments were carried out. The experimental results demonstrated that the piezoelectric fiber with a metal core functions effectively as a sensor or actuator for active vibration control, and our control design method resolved the actuator unevenness issue.

2. MODELING

2.1. Finite-element modeling

A CFRP smart board embedded with metal-core piezoelectric fibers is used as a cantilever beam in this paper. The origin of the x–y–z axes is centered as shown in Figs 1 and 2. The full-order model is derived by using the finite-element method. $n+1$ piezoelectric fibers are embedded in the CFRP composite. One of the fibers is used as a sensor and n fibers are utilized as actuators. Torsional vibration of the beam is negligible, and there are 18 elements. The elements are numbered 1 to 18 from left to right. L is the length of the element. Using the shape function obtained in Ref. [6]

$$w_i(x_i,t) = \left(1 - 3\frac{x_i^2}{L^2} + 2\frac{x_i^3}{L^3}\right) y_{i-1}(t) + \left(\frac{x_i}{L} - 2\frac{x_i^2}{L^2} + \frac{x_i^3}{L^3}\right) L v_{i-1}(t) + \left(3\frac{x_i^2}{L^2} - 2\frac{x_i^3}{L^3}\right) y_i(t) - \left(\frac{x_i^2}{L^2} - \frac{x_i^3}{L^3}\right) L v_i(t), \tag{1}$$

and the stiffness matrix and the mass matrix of the beam are computed as follows:

$$[K] = \frac{EI}{L^3} \begin{bmatrix} 12 & 6L & -12 & 6L \\ 6L & 4L^2 & -6L & 2L^2 \\ -12 & -6L & 12 & -6L \\ 6L & 2L^2 & -6L & 4L^2 \end{bmatrix}, \tag{2}$$

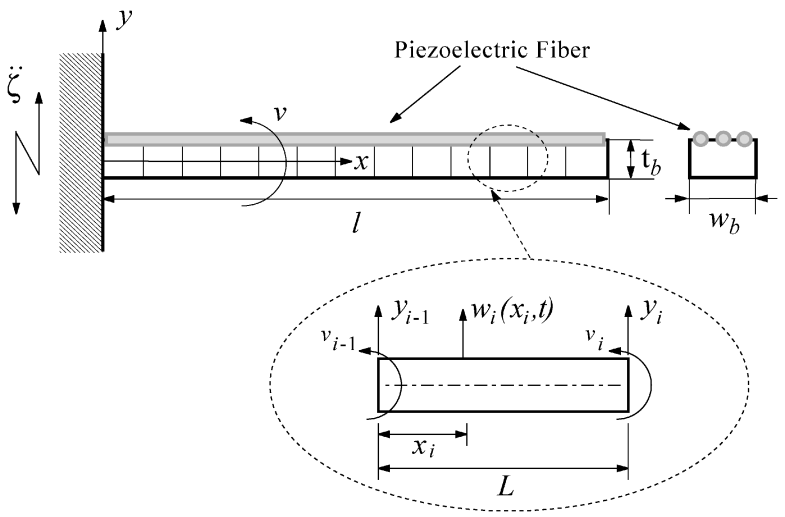

Figure 1. Model of CFRP board mounting piezoelectric fiber.

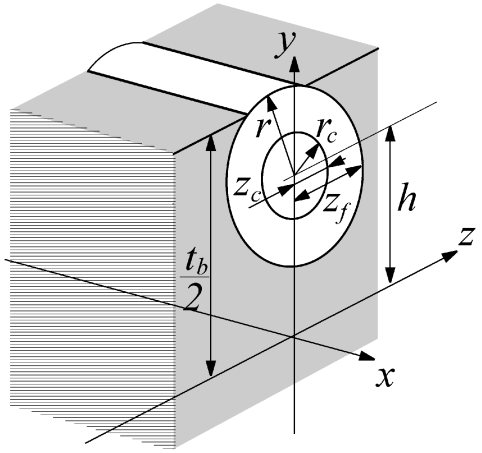

Figure 2. Metal core assisted piezoelectric fiber.

$$[M] = \frac{mL}{420}\begin{bmatrix} 156 & 22L & 54 & -13L \\ 22L & 4L^2 & 13L & -3L \\ 54 & 13L & 156 & -22L \\ -13L & -3L^2 & -22L & 4L^2 \end{bmatrix}. \tag{3}$$

Next, the distributed moment that the metal-core piezoelectric fibers applies to the beam as an actuator is derived. When an electric field is applied between the metal core and the surface of the PZT ceramics, the piezoelectric fibers expand and contract in the longitudinal direction. The expansion and contraction of the piezoelectric fibers creates longitudinal bending stress in the CFRP beam.

If a voltage V is applied to the piezoelectric fiber, the piezoelectric strain ε is

$$\varepsilon = \frac{d_{31}}{r - r_c} V. \tag{4}$$

This strain results in a longitudinal stress σ given by

$$\sigma = E_a \varepsilon = E_a \frac{d_{31}}{r - r_c} V. \tag{5}$$

The moment applied by the piezoelectric fiber to the beam is derived as follows:

$$\begin{aligned} M_a &= \int_{h-r}^{h-r_c} 2\sigma z_f y \, \mathrm{d}y + \int_{h+r_c}^{h+r} 2\sigma z_f y \, \mathrm{d}y \\ &\quad + \int_{h-r_c}^{h+r_c} \{2\sigma (z_f - z_c) - 2E_p \varepsilon z_c\} y \, \mathrm{d}y \\ &= d_{31} h \pi \frac{E_a r^2 - (E_a + E_p) r_c^2}{r - r_c} V, \end{aligned} \tag{6}$$

where z_f, z_c are

$$z_f = \sqrt{r^2 - (y - h)^2}, \tag{7}$$

$$z_c = \sqrt{r_c^2 - (y - h)^2}. \tag{8}$$

The actuator constant C_a is defined as below

$$M_a = C_a V. \tag{9}$$

The metal-core piezoelectric fibers each have unevenness in the actuator constant. Possible reasons for this are:

(1) Nonuniformity in the piezoelectric strain because of the very small gap from a center of the metal core,

(2) Individual differences of the ceramics arising from the sintering condition in fabricating the piezoelectric fiber, and

(3) Effect of the interface between CFRP composite and piezoelectric fiber.

The coefficient α_i is introduced considering these reasons. The moment M_{ai} that the ith piezoelectric fiber applies to the beam is

$$M_{ai} = \alpha_i C_a V_i, \quad i = 1, \ldots, n, \tag{10}$$

where V_i denotes the voltage applied ith piezoelectric fiber. The coefficients α_i are shown in Fig. 3. The coefficients α_i are experimentally identified by applying voltage V_i at a first-mode frequency and by 4SID method of the system identification theory. The bending moment M_{ai} is applied to the tip of the cantilever because piezoelectric fibers are embedded in the 18 elements. We determine the damping

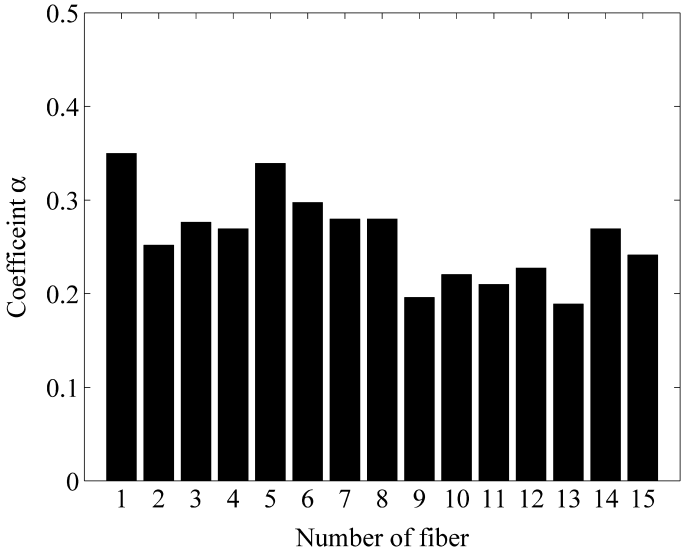

Figure 3. Coefficent of α_i.

matrix C from the time-history response:

$$C = 6.0 \cdot 10^{-5} M + 1.1 \cdot 10^{-5} K. \tag{11}$$

Hence, the governing equation is

$$M\ddot{\mathbf{x}} + C\dot{\mathbf{x}} + K\mathbf{x} = F\mathbf{u} - H\ddot{\zeta}, \tag{12}$$

$$\mathbf{x} = [y_1 v_1 \ \dots \ y_i v_i \ \dots \ y_{18} v_{18}]^{\mathrm{T}}, \tag{13}$$

$$F = [0 \ \dots \ 0 \ C_a]^{\mathrm{T}} [\alpha_1 \dots \alpha_n], \tag{14}$$

$$\mathbf{u} = [V_1 \cdots V_n]^{\mathrm{T}}, \tag{15}$$

$$H = \frac{mL}{18} [1 \ 0 \ \dots \ 1 \ 0 \ \dots \ 1 \ 0]^{\mathrm{T}}, \tag{16}$$

where we define the disturbance input vector H on the assumption that the beam is excited by an external disturbance from the fixed end depending on the absolute acceleration $\ddot{\zeta}$.

When the piezoelectric fiber is used as a sensor, the sensor voltage V_s is produced by the strain in the piezoelectric fiber [10]. The sensor constant K_s is approximated under the assumption that the charge developed on the piezoelectric fiber is equivalent to the piezoelectric plate, which has the same width as the circumference of the metal core.

$$\begin{aligned} V_s &= \frac{\alpha_s}{C_p} \int_0^l E_a h d_{31} 2\pi r_c \frac{\partial y(x,t)}{\partial x^2} \, \mathrm{d}x \\ &= \frac{2\pi E_a h d_{31} r_c y'(l)}{C_p} = K_s y'(l) \end{aligned} \tag{17}$$

where y' is the spatial derivative of y and α_s is a coefficient identified experimentally to be the same as α_i.

The state equation and the output equation of the full-order model are obtained

$$\dot{\mathbf{x}}_f = A_f \mathbf{x}_f + B_{fz}\ddot{\zeta} + B_{fu}\mathbf{u}, \tag{18}$$

$$\mathbf{y}_f = [\,\mathbf{0}_{1\times 35} \quad K_s \quad \mathbf{0}_{1\times 36}\,]\mathbf{x}_f = C_f \mathbf{x}_f, \tag{19}$$

where the state vector $\mathbf{x}_f$, the system matrix A_f and the input matrices B_{fz} and B_{fu} are

$$\mathbf{x}_f = [\,\mathbf{x} \quad \dot{\mathbf{x}}\,]^{\mathrm{T}}, \tag{20}$$

$$A_f = \begin{bmatrix} \mathbf{0} & \mathbf{I} \\ -M^{-1}K & -M^{-1}C \end{bmatrix},$$

$$B_{fz} = \begin{bmatrix} \mathbf{0} \\ -M^{-1}H \end{bmatrix}, \quad B_{fu} = \begin{bmatrix} \mathbf{0} \\ M^{-1}F \end{bmatrix}. \tag{21}$$

2.2. Control design model

This study is conducted on the active control of the first mode of a cantilevered beam using piezoelectric fibers as the sensor and actuator. The reduced-order model for the controller design is obtained by using the modal-truncation method to focus on the first mode from (18). We introduce the matrices T and S

$$T = \begin{bmatrix} \Phi & \mathbf{0}_{36\times 36} \\ \mathbf{0}_{36\times 36} & \Phi \end{bmatrix}, \quad S = \begin{bmatrix} 1\ \mathbf{0}_{1\times 35} & \mathbf{0}_{1\times 36} \\ \mathbf{0}_{1\times 36} & 1\ \mathbf{0}_{1\times 35} \end{bmatrix} \tag{22}$$

where the matrix $\Phi = [\phi_1\ \phi_2\ \ldots\ \phi_{36}]$ consists of the ith mode vector ϕ_i. Defining q_i as the modal coordinates of the ith mode, we obtain the reduced-order model considering the first mode only as follows.

$$\dot{\mathbf{x}}_r = A_r \mathbf{x}_r + B_{rz}\ddot{\zeta} + B_{ru}\mathbf{u}, \quad \mathbf{x}_r = [q_1 \dot{q}_1]^T, \tag{23}$$

$$\mathbf{y}_r = C_r \mathbf{x}_r, \tag{24}$$

$$A_r = ST^{-1}A_f T S^T, \quad B_{rz} = ST^{-1}B_{fz},$$

$$B_{ru} = ST^{-1}B_{fu}, \quad C_r = C_f T S^T.$$

In this study, n piezoelectric fibers are driven with a single piezo amplifier; the same voltage is thus applied to the piezoelectric fibers. Therefore, a single-input model is needed for the control design. Hence, the LFT is formulated considering the unevenness of actuator coefficients as the perturbation from the reduced-order model (23). This paper denotes an upper LFT X and Y as $X \otimes Y$. An upper LFT is defined as:

$$X \otimes Y := Y_{22} + Y_{21}X(I - XY_{11})^{-1}Y_{12}. \tag{25}$$

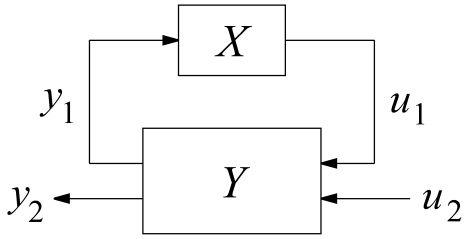

Figure 4. LFT $X \otimes Y$.

$X \otimes Y$ is the transfer function from u_2 to y_2 including the matrix X: $u_1 = Xy_1$ as illustrated in Fig. 4 where the matrix Y is partitioned as

$$\begin{bmatrix} y_1 \\ y_2 \end{bmatrix} = \begin{bmatrix} Y_{11} & Y_{12} \\ Y_{21} & Y_{22} \end{bmatrix} \begin{bmatrix} u_1 \\ u_2 \end{bmatrix}. \tag{26}$$

Elements of the matrix B_{ru} of (23) are obtained as follows.

$$B_{ru} = \begin{bmatrix} 0 & \cdots & 0 \\ \beta_1 & \cdots & \beta_n \end{bmatrix}. \tag{27}$$

The range of $\beta_i (i = 1, \ldots, n)$ becomes

$$\beta_N - \delta\Delta_b \leqslant \beta_i \leqslant \beta_N + \delta\Delta_b, \tag{28}$$

where the nominal values β_N and Δ_b are computed as follows:

$$\beta_N = \frac{\max(\beta_i) - \min(\beta_i)}{2}, \tag{29}$$

$$\Delta_b = \frac{\max(\beta_i) - \beta_N}{2}. \tag{30}$$

Matrix B_{ru} is replaced by the following matrix:

$$B_{ru} = \begin{bmatrix} 0 \\ \beta_N \end{bmatrix} + \delta \begin{bmatrix} 0 \\ \Delta_b \end{bmatrix} = B_n + \delta B_1, \tag{31}$$

$$|\delta| < 1. \tag{32}$$

The state equation of the reduced-order model is rewritten as follows:

$$\dot{x}_r = A_r x + (\hat{B}_n + \delta\hat{B}_1)[\ddot{\zeta}\ u]^{\mathrm{T}}, \tag{33}$$

where

$$\hat{B}_n = [B_{rz}\ B_n], \quad \hat{B}_1 = [0\ B_1]. \tag{34}$$

After the matrix $[\mathbf{0}\ \mathbf{0}\ \hat{B}_1]$ is decomposed into matrices [11] $L \in \Re^{2\times 1}$, $[R\ W\ Z] \in \Re^{1\times 6}$,

$$[\mathbf{0}\ \mathbf{0}\ \hat{B}_1] = [L] \times [R\ W\ Z], \tag{35}$$

Table 1.
Specifications of model

l	0.17 (m)
EI	7.63×10^{-2} (N m^2)
w_b	0.027 (m)
t_b	0.0011 (m)
r	100×10^{-6} (m)
r_c	25×10^{-6} (m)
h	0.45×10^{-3} (m)
E_a	25×10^{9} (Pa)
E_p	1.68×10^{11} (Pa)
d_{31}	-260×10^{-12} (m/V)
C_p	2.2×10^{-9} (F)
α_s	0.51
n	29

the LFT representation is obtained as follows [11]:

$$y = \delta \otimes G[\ddot{\zeta}\ u]^{\mathrm{T}}, \tag{36}$$

where

$$G := \left[\begin{array}{c|cc} A_r & L & \hat{B}_n \\ \hline W - RA_r & -RL & Z - R\hat{B}_n \\ C_r & 0 & 0 \end{array}\right]. \tag{37}$$

Table 1 shows the specifications of the model.

3. CONTROL SYSTEM DESIGN

This section designs the control system that considers the perturbation caused by the unevenness of actuator coefficients using μ synthesis. The generalized plant is presented as Fig. 5. $\delta \otimes G$ denotes the LFT representation (37). Input disturbances w_{11}, w_{12} and controlled variables z_{11}, z_{12} are added. The term W_1 is the weighting function for maintaining the stability of the higher modes and high-frequency noise. W_1 is chosen to cover the multiplicative error Δ_w that is estimated between the finite-element model and the reduced-order model. W_2 is the weighting function for the control performance. We add a slight peak in W_2 to improve the control performance of the first mode frequency. The robust control performance in μ synthesis can result in a problem in robust stabilization when virtual perturbation Δ_w is introduced between z_{11}, z_{12} and w_{11}, w_{12}. Figure 6 illustrates the gain diagram of weighting functions and the multiple error Δ_p. The sixth-order controller is obtained by three D-K iterations. Figure 7 displays the bode diagram of the controller. However, the controller has a peak around the first mode of the beam, but the controller gain is low enough in the higher frequency

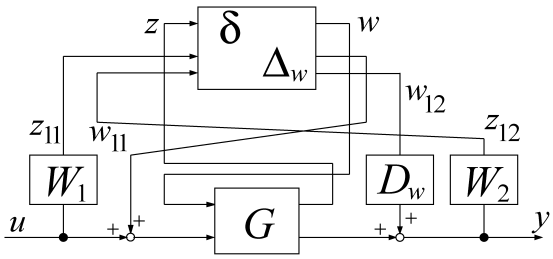

Figure 5. Generalized plant.

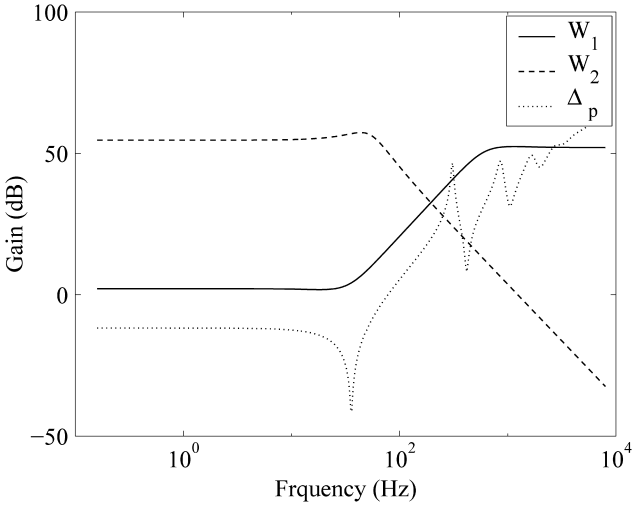

Figure 6. Gain diagram of weighting function.

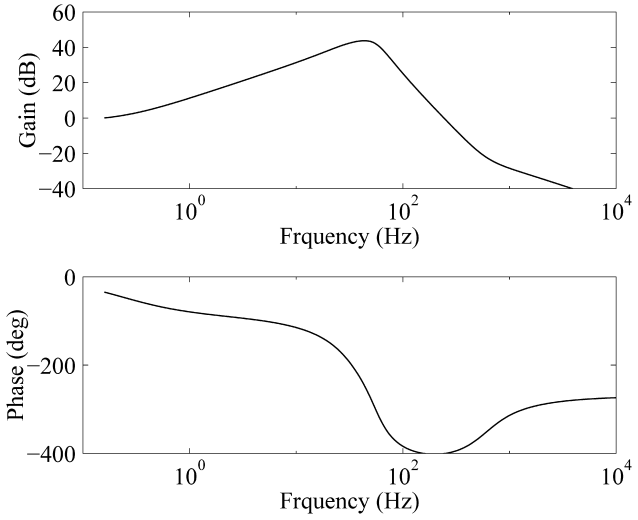

Figure 7. Bode diagram of controller.

domain. Therefore, the controller is robust with respect to the truncated high-frequency modes or high-frequency noise.

4. EXPERIMENTAL

4.1. Experimental setup

The extrusion method is used for fabricating the piezoelectric fiber. PZT powder was mixed with binder and water and the resulting paste was extruded from a 220 μm bore diameter nozzle with a platinum fine line of 50 μm diameter. After drying at room temperature, continuous defatting and sintering were performed in a movable furnace by moving the furnace from the end of the fiber. Next, piezoelectric fibers were embedded in the CFRP composite. Piezoelectric fibers were placed on the six layers-stacking of CFRP prepregs $[0_2/90_2/0_2]$. The stacking was pressed under 0.3 MPa at 135°C for 2 hours by using a hot press.

Figure 8 illustrates the schematic diagram of the experimental setup of the active vibration control. As the piezoelectric fiber in the CFRP board expands and contracts, corresponding to the bending of the board, an electric charge is generated from the piezoelectric fiber. The generated voltage is acquired using an A/D and D/A converter Contec ADA16-32/2(PCI)F on a computer through a voltage follower (impedance transformer). The continuous controller designed in Section 3 is digitized with a sampling time of 1 ms. After the control input is computed, all piezoelectric fibers are driven by an NF Electronic Instruments piezo driver 4005 as actuators. A Keyence LK-2000 laser displacement sensor is used to measure the displacement of the tip of the beam.

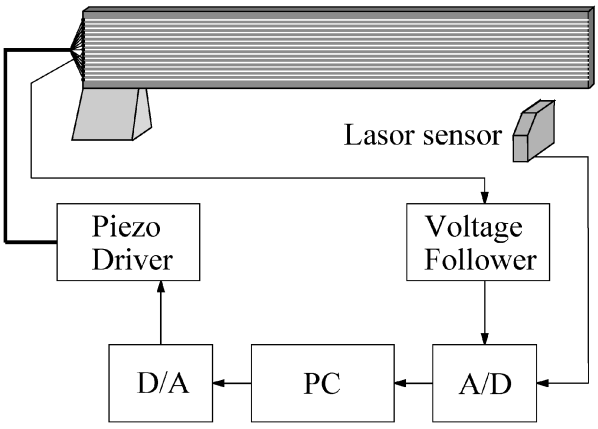

Figure 8. Experimental setup.

4.2. Experimental results

We performed the active vibration control experiments of the CFRP composite beam by using piezoelectric fibers as a sensor and actuators. Figure 9(a) demonstrates the displacement of the beam tip; Fig. 9(b) illustrates the sensor output of the piezoelectric fiber; and Fig. 9(c) shows the control input. The disturbance is generated before starting the control by inducing a vibration through the application of ±50 V for a second at a first mode frequency. The solid line indicates the

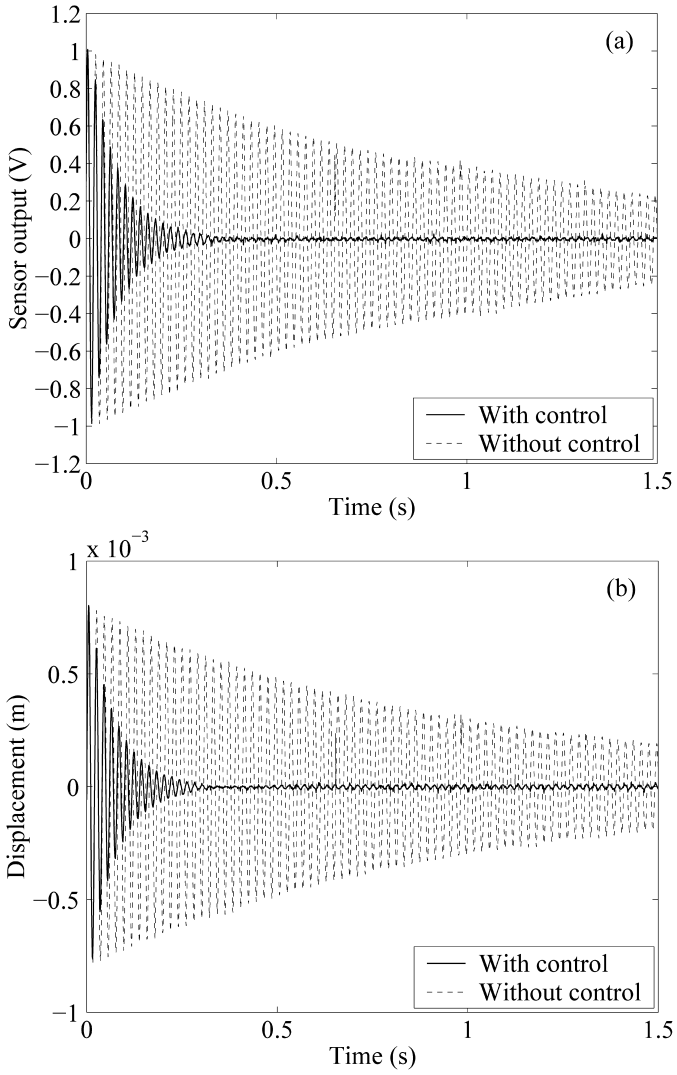

Figure 9. Experimental results: (a) sensor output (V); (b) displacement of tip (m); (c) control input (V).

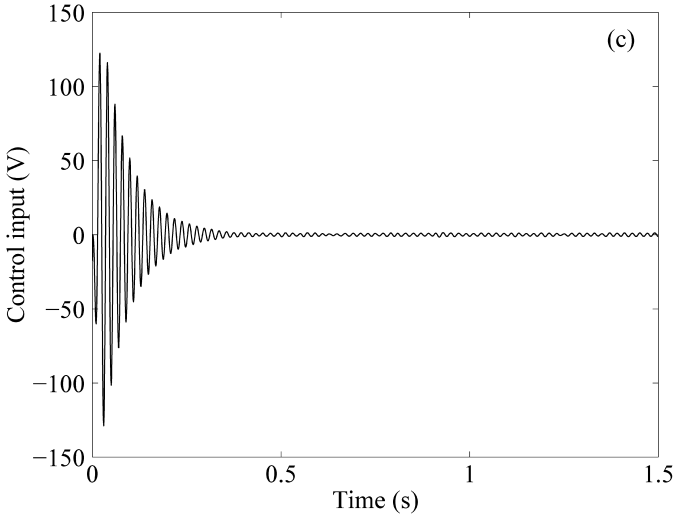

Figure 9. (Continued).

response with control, and the broken line indicates response without control. The feedback controller uses the sensor output of the piezoelectric fiber shown in Fig. 9(a). Figure 9(b) indicates that the vibration of the beam tip is effectively suppressed by our control system. Figure 10 outlines the experimental results of frequency responses. Attenuations of about 10 dB are achieved by using our control system. Vibration is not suppressed in the second and third modes because we consider vibration suppression of the first mode only. However, our controller does not destabilize higher frequency modes; the spillover phenomenon is thus not present. Therefore, it is obvious that our controller is robustly stable for the truncated high-frequency modes. When a controller for the second and the third modes is required, a robust controller is designed by using the reduced-order model considering up to the third mode after the multiplicative error is estimated between the finite-element model and the reduced-order model.

Next, the control performance of the controller using μ synthesis is compared to that of an H_∞ controller designed without considering the actuator unevenness. The maximum value of the control input of the H_∞ controller is the same as that of the controller using μ synthesis. However, the difference is not so large, because the control performance is scarcely affected by the unevenness of the actuator when there are few piezoelectric fibers. For this reason, we carried out the simulation of the smart beam embedding 240 piezoelectric fibers. Figure 11 presents the simulation results. The solid line indicates the response with μ control, and the broken line indicates response with H_∞ control. The controller using μ synthesis is seen to suppress the vibration quicker than the H_∞ controller because in the μ synthesis the gain of the controller is optimized considering the unevenness of the actuator coefficient.

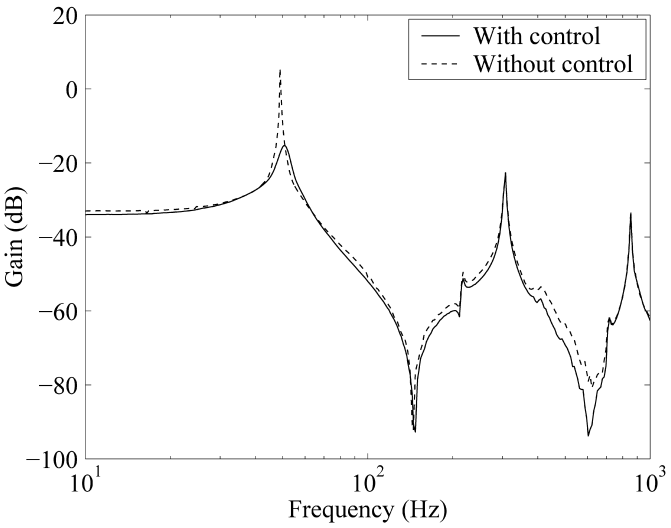

Figure 10. Experimental reslut of frequency responses.

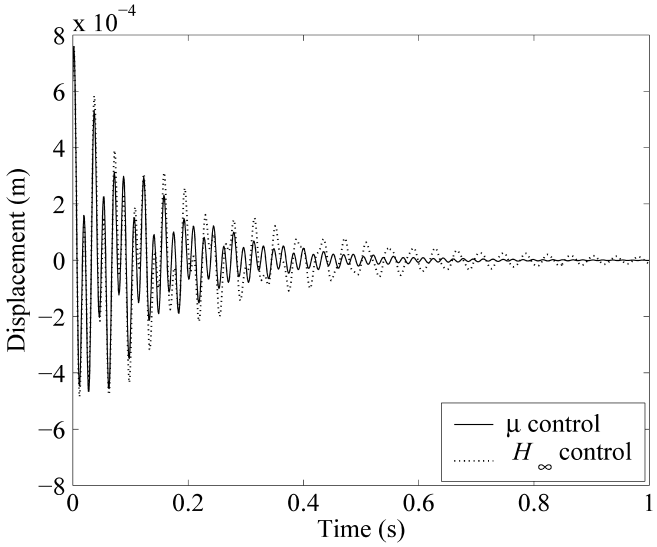

Figure 11. Comparison between μ and H_∞ controller.

5. CONCLUSION

This paper described the active vibration control of a smart beam containing piezoelectric fibers with metal cores that function as sensors and actuators in the CFRP composite. A finite-element model and a reduced-order model for controller design were established. Furthermore, the reduced-order model was transformed into a LFT representation considering the actuator unevenness as the perturbation. Next, a controller using μ synthesis was designed. The experimental results

demonstrated that a piezoelectric fiber with a metal core functions as the sensor or the actuator for effectively controlling active vibration, and our control design method overcomes the problem of actuator unevenness. In future work, we plan to utilize piezoelectric fiber as a sensor or an actuator for torsional vibration. We will design the controller for torsional vibration in addition to bending vibration. Applications such as helicopter blades can then be anticipated.

REFERENCES

1. S. V. Gosavi and A. G. Kelkar, Passivity-based robust control of piezo-actuated flexible beam, in: *Proceedings of the 2001 American Control Conference*, 2493–2497 (2001).
2. K. Ohima, T. Takigami and Y. Hayakawa, Robust vibration control of a cantilever beam using self-sensing actuator, *JSME Intern. J. Serial C* **40**, 681–687 (1997).
3. M. Okugawa and M. Sasaki, System identification and controller design of a self-sensing piezoelectric cantilever structure, in: *Proceedings of SPIE* **4326**, 34–45 (2001).
4. I. Kajiwara and M. Uehara, Design of shape and control system for smart structures with piezoelectric films, in: *Proceedings of AIAA, 42nd SDM Conference*, CD-ROM (No. 2001-1555) (2001).
5. A. A. Bent, N. Hagood and J. Rodgers, Anisotropic actuation with piezoelectric fiber composites, *J. Intelligent Mater. Systems Structures* **6**, 338–349 (1995).
6. L. Meirovitch, *Elements of Vibration Analysis*, McGraw-Hill, New York, pp. 300–346 (1986).
7. H. Sato, Y. Shimojo and T. Sekiya, Development of metal core-assisted piezoelectric complex fibers and application to the smart board, *Trans. Jpn. Soc. Mech. Eng.* (in Japanese) **69A**, 1305–1310 (2003).
8. H. Sato, Y. Shimojo and T. Sekiya, Development of the piezoelectric fiber and application for the smart board, in: *Proceedings of ISSS- SPIE 2002* pp. 242–246 (2002).
9. A. Baz and S. Poh, Performance of an active control system with piezoelectric actuators, *J. Sound Vibration* **126**, 327–343 (1998).
10. J. J. Dosch, D. J. Inman and E. Garcia, A self-sensing piezoelectric actuator for collocated control, *J. Intell. Mater. Syst. Struct.* **3**, 166–185 (1992).
11. M. Hirata, K. Z. Liu and T. Mita, Active vibration control of a 2-mass system using μ-synthesis with a descriptor form representation, *Control Eng. Practice* **4**, 545–552 (1996).